Step Height Measurement by Using Heterodyne Central Fringe Identification Technique

W. T. Wu*, H. C. Hsieh, Y. L. Chen, W. Y. Chang, and D. C. Su
Department of Photonics and Institute of Electro-Optical Engineering, National Chiao-Tung University, 1001 Ta-Hsueh Road, Hsinchu 30050, Taiwan, ROC

ABSTRACT

A simple method for measuring a step-height sample is presented with the heterodyne central fringe identification technique and a precision translation stage. This method can accurately point out the zero optical path difference position such that the optical path lengths of two arms of the interferometer are absolutely equivalent. Thus, the two surfaces of the step-height sample can be identified sequentially with the translation stage. The displacement of the translation stage is equal to the step-height of the test sample. The feasibility of the technique is demonstrated. The measurable range is not limited by the coherence length of the light source. The measurement accuracy depends on the uncertainties of the heterodyne central fringe identification method and the translation stage. In our setup, we have a 100 mm measurable range and a 4 nm uncertainty. The wavelength stability of the light source has a minor effect on the measurement.

Keywords: central fringe, heterodyne interferometry, electro-optic modulator, tunable laser, translation stage, step-height.

1. INTRODUCTION

The accurate length measurement technique is very basic and important in science researches and industrial products. It will affect the research results and the product qualities. The interferometer with a laser light source can obtain very good results in wavelength unit and it is also a non-destructive technique, so it is often used for the accurate length measurement. On the other hand, the lengths of two arms of the Michelson interferometer [1] with white light source can set to be equal as the maximum intensities of the interference fringes are appeared. That technique is known as the central fringe identification technique [2-7]. The resolution is about 1~2 μm. To enhance the measurement resolution, Lee *et al*. [8] proposed an improved method with the heterodyne interferometry [9-12]. This method can accurately point out the zero optical path difference position such that the optical path lengths of two arms of the interferometer are absolutely equivalent.

In this paper, a simple method for measuring a step-height sample is presented with the wavelength scanning heterodyne central fringe identification technique and a precision translation stage. It can more easily identify the moving direction and phase variation (can exceed 2π) of interference fringes to induce the required moving direction and almost distance of reference mirror for the zero optical path difference position. In the measuring procedure, first, one surface of the step-height sample can be identified when the lengths of two arms are equal. Secondly, the reference mirror is displaced with the translation stage and another surface of the tested sample can be identified similarly. The displacement of the translation stage is equal to the step-height of the test sample. The feasibility of the technique is demonstrated. The measurable range is not limited by the coherence length of the light source. The measurement accuracy depends on the uncertainties of the heterodyne central fringe identification method and the translation stage. In our setup, we have a 100 mm measurable range and a 4 nm uncertainty. The wavelength stability of the light source has a minor effect on the measurement. Hence, it has some merits such as high accuracy, long measuring range, simple optical structure, and easy operation.

*wuwonds@gmail.com; phone +886-3-573-1951; fax +886-3-571-6631

Instrumentation, Metrology, and Standards for Nanomanufacturing IV, edited by Michael T. Postek, John A. Allgair,
Proc. of SPIE Vol. 7767, 77670J · © 2010 SPIE · CCC code: 0277-786X/10/$18 · doi: 10.1117/12.860356

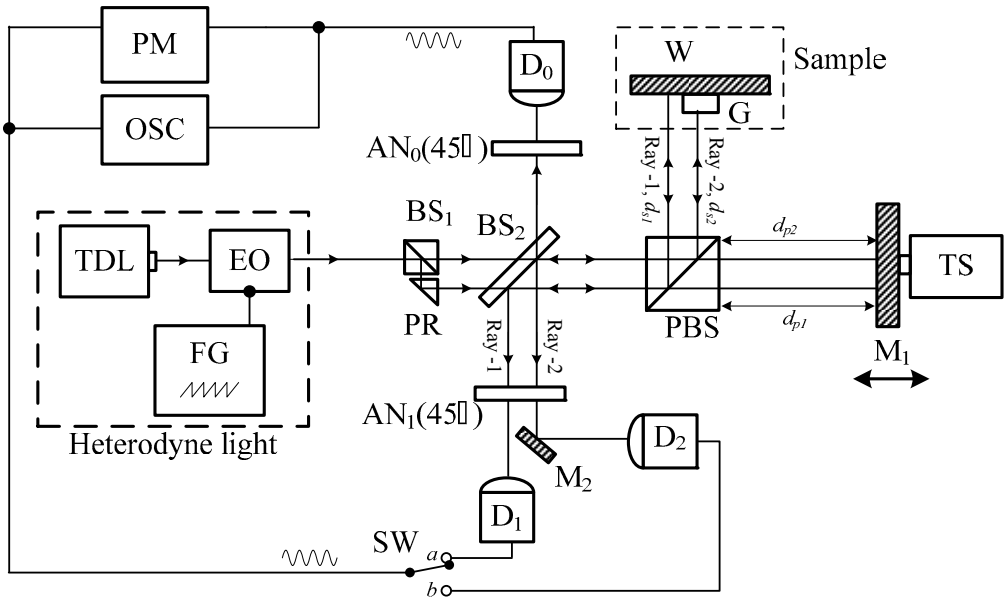

Fig. 1. The schematic diagram of this method. TDL, tunable diode laser; EO, electro-optic modulator; FG, function generator; BS, beam splitter; PR, prism; PBS, polarizing beam splitter; G, gauge block; W, wringing platen; M, mirror; TS, translation stage; AN, analyzer; D, photo-detector; SW, switch; OSC, oscilloscope; PM, phase-meter.

2. PRINCIPLE

The schematic diagram of this method is shown in Fig. 1. For convenience, the +z-axis is chosen to be along the light propagation direction and the +y-axis is the direction pointing out the paper plane. The Jones vector [13] of a linear polarized light from the tunable diode laser (TDL) at an angle of 45º with respect to the x-axis can be written as

$$E_{in} = \frac{1}{\sqrt{2}}\begin{bmatrix}1\\1\end{bmatrix}. \tag{1}$$

This light passes through an electro-optic modulator (EO) whose fast axis is along x-axis. An external sawtooth voltage signal with an angular frequency ω and an amplitude V_π, the half-wave voltage of the EO, is applied to the EO by using the function generator (FG). Hence there is an angular frequency difference ω between its s- and p- polarizations, and it becomes a heterodyne light. This light beam passes through the beam splitter (BS_1) and the prism (PR), and is divided into two parallel light beams Ray-1 and Ray-2. Then they enter into a modified Michelson interferometer which consists of a beam splitters (BS_2), a polarization beam splitter (PBS), two mirrors (M), a translation stage (TS), a gauge block (G), a wringing platen (W), two analyzers (AN), and three photo-detectors (D). The G is wrung on the W as a test sample and the M_1 is a reference mirror translated by the translation stage (TS). The optical paths of Ray-1 are PBS→ W→ PBS→ BS_2→ AN_1→ D_1 (s-polarization) and PBS→ M_1→ PBS→ BS_2→ AN_1→ D_1 (p-polarization). The optical paths of Ray-2 are PBS→ G→ PBS→ BS_2→ AN_1→ D_2 (s-polarization) and PBS→ M_1→ PBS→ BS_2→ AN_1→ D_2 (p-polarization).

These beams pass through the AN_1 with the transmission axis at 45° to the x-axis. Using the Jones calculus, the Jones vectors of the s- and p- polarization light before entering into the $D_{i\,(i=1,2)}$ can be derived and written as

$$
\begin{aligned}
E_{si} &= AN(45°)\cdot 2d_{si}\cdot R_{PBS}\cdot EO(\omega t,0°)\cdot E(45°) \\
&= \frac{1}{2}\begin{bmatrix}1 & 1\\ 1 & 1\end{bmatrix}\cdot e^{j\frac{4\pi d_{si}}{\lambda}}\cdot\begin{bmatrix}0 & 0\\ 0 & 1\end{bmatrix}\cdot\begin{bmatrix}e^{j\frac{\omega t}{2}} & 0\\ 0 & e^{-j\frac{\omega t}{2}}\end{bmatrix}\cdot\frac{1}{\sqrt{2}}\begin{bmatrix}1\\ 1\end{bmatrix} \\
&= \frac{1}{2\sqrt{2}}\begin{bmatrix}1\\ 1\end{bmatrix}e^{j\{\frac{4\pi d_{si}}{\lambda}-\frac{\omega t}{2}\}}\quad,\quad (i=1,2)
\end{aligned}
\tag{2}
$$

and

$$
\begin{aligned}
E_{pi} &= AN(45°)\cdot 2d_{pi}\cdot T_{PBS}\cdot EO(\omega t,0°)\cdot E(45°) \\
&= \frac{1}{2}\begin{bmatrix}1 & 1\\ 1 & 1\end{bmatrix}\cdot e^{j\frac{4\pi d_{pi}}{\lambda}}\cdot\begin{bmatrix}1 & 0\\ 0 & 0\end{bmatrix}\cdot\begin{bmatrix}e^{j\frac{\omega t}{2}} & 0\\ 0 & e^{-j\frac{\omega t}{2}}\end{bmatrix}\cdot\frac{1}{\sqrt{2}}\begin{bmatrix}1\\ 1\end{bmatrix} \\
&= \frac{1}{2\sqrt{2}}\begin{bmatrix}1\\ 1\end{bmatrix}e^{j(\frac{4\pi d_{pi}}{\lambda}+\frac{\omega t}{2})}\quad,\quad (i=1,2)
\end{aligned}
\tag{3}
$$

where R_{PBS} and T_{PBS} are the transformation matrices of the PBS for the reflected light and the transmitted light respectively; λ is the wavelength of the light; d_{pi} and d_{si} are optical path lengths of two arms in the interferometer; the subscript i (i=1, 2) refers to Ray-1 and Ray-2, respectively. Then the light intensity received by the D_i can be written as

$$
I_i = \left|E_{si}+E_{pi}\right|^2 = \frac{1}{2}[1+\cos(\omega t+\phi_i)],\ (i=1,\ 2) \tag{4}
$$

where the phase is

$$
\phi_i = \frac{4\pi d_i}{\lambda}\,. \tag{5}
$$

Here d_i ($d_i \equiv d_{pi}-d_{si}$) is the optical path difference between two arms.

Also, another heterodyne light beam reflected by the BS_2 passes through the AN_0 with the transmission axis at 45° to the x-axis and enters the D_0. Its electric field and intensity have the forms as

$$
\begin{aligned}
E_r &= AN(45°)\cdot EO(\omega t,0°)\cdot E(45°) \\
&= \frac{1}{2}\begin{bmatrix}1 & 1\\ 1 & 1\end{bmatrix}\cdot\begin{bmatrix}e^{j\frac{\omega t}{2}} & 0\\ 0 & e^{-j\frac{\omega t}{2}}\end{bmatrix}\cdot\frac{1}{\sqrt{2}}\begin{bmatrix}1\\ 1\end{bmatrix} \\
&= \frac{1}{\sqrt{2}}\begin{bmatrix}1\\ 1\end{bmatrix}\cos(\omega t/2)\qquad\quad,
\end{aligned}
\tag{6}
$$

and

$$
I_r = \left|E_r\right|^2 = \frac{1}{2}[1+\cos(\omega t)]\,. \tag{7}
$$

I_r is the reference signal. Both I_r and I_i are sent into the phase-meter (PM), from which the phase ϕ_i can be obtained.

When the wavelength of the light is changed from λ_1 to λ_2, there is a phase variation $\Delta\phi_i$ which can be derived from Eq. (5) and written as

$$\Delta\phi_i = \phi_{i,\lambda_2} - \phi_{i,\lambda_1} = \frac{4\pi d_i \Delta\lambda}{\lambda_1 \lambda_2}, \tag{8}$$

where $\Delta\lambda \equiv \lambda_2 - \lambda_1$. From Eq. (8), it is obvious that only if the optical lengths of the two arms in the interferometer are equivalent, i.e., $d_i = 0$, then $\Delta\phi_i$ equals zero despite the wavelength variation. This is the core concept of the heterodyne central fringe identification technique. Consequently, the M_1 can be accurately positioned where the optical paths of two arms of the interferometer are absolutely equivalent with the heterodyne central fringe identification technique. In Fig. 2, if Ray-1 is considered first, then the position of M_1 is identified as the corresponding position of the W and it is denoted as W' such that $d_{p1} = d_{s1}$. Afterward the M_1 is displaced by the TS along the optical axis until it is positioned the exact position where the optical paths of two arms of the interferometer are absolutely equivalent again for Ray-2 with the same technique. Here, this position of M_1 is identified as the corresponding position of the G and it is denoted as G' such that $d_{p2} = d_{s2}$. The displacement of the M from W' to G' can be obtained by reading the data of the TS and it is equal to the step-height L of the sample.

3. EXPERIMENTS

In order to show the validity of this method, a tunable diode laser (Model 6304, New Focus) with a wavelength tuning range of 632.60~637.96 nm and a tuning resolution of 0.02 nm is used. The gauge block (Mitutoyo, No. 516-402-26) of 1.03 mm is in grade 0 [14]. The M_1 is displaced by a precision translation stage (Chuo Precision, ALS-510-H1P) and its position is read with an optical meter (Sony, BL57-NE). The stage has a minimum incremental motion of 1 nm and a maximum travel range of 100 mm. The EO (Model 4002, New Focus) driven by the saw-tooth signal with a frequency of 500 Hz and a phase-meter with a uncertainty of 0.036° is also introduced. The reading of the phase-meter and the direction and wave numbers of the sine wave signals displayed on the oscilloscope (OSC) are used to identify the position of the M_1. That is, as $\Delta\phi_i > 0$, it means the M_1 do not reach the zero optical path difference position yet; as $\Delta\phi_i < 0$, it means the M_1 already exceeds the zero optical path difference position. Moreover, the corresponding optical path difference d_i can be estimated by using Eq. (8). The following procedures are operated and the associated data in our tests are listed in Table 1.

I. In order to determine the zero optical path difference position W' of the wringing platen, first, the M_1 is slightly located behind W' (see Fig. 2) by a ruler for a convenient measurement and the switch (SW) is turned to the position *a* for Ray-1. When the wavelength of the light scans from λ_1 to λ_2, we can see the point A of signal I_1 shifts to the point B on the OSC, in which I_r is the reference signal as shown in Fig. 3. Let $\Delta\lambda$ be a minimum, then the phase variation $\Delta\phi_1$ displayed on the PM is recorded as 18.09°. Because the sine wave signals displayed on the OSC is displaced over one period, $\Delta\phi_1$ must be modified as 369.20°. The data of d_1 is derived from Eq. (8), and the translation stage is displaced forward 10.3 mm.

II. Increase the amount of $\Delta\lambda$, and repeat the step I, then we find that $\Delta\phi_1$ becomes negative. It means the M_1 has exceeded the position W' and the TS should be moved back 26.5 μm.

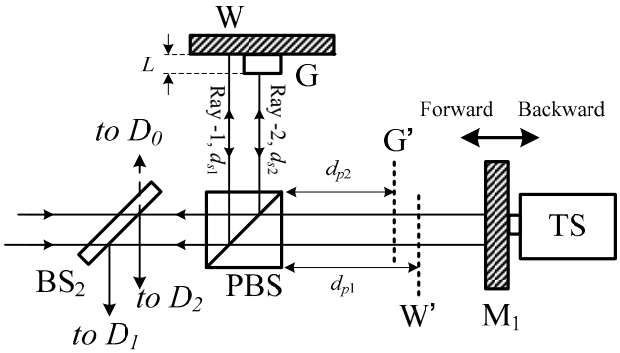

Fig. 2 Modified Michelson interferometer.

Table 1. Experimental condition and its associated data at each step (at 20°C).

	λ_1 [nm]	λ_2 [nm]	$\Delta\lambda$ [nm]	$\Delta\phi_1$ [deg.]	$d_1 = \Delta\phi_1 \frac{\lambda_1\lambda_2}{4\pi\Delta\lambda}$	stage displacement
I	633.00	633.02	0.02	369.20	1.0274E+07	10300000 nm
II	633.00	634.00	1.00	-47.51	-2.6482E+04	-26500 nm
III	632.60	637.96	5.36	0.15	1.6000E+01	16 nm
IV	632.60	637.96	5.36	0	0.0000E+00	
	λ_1 [nm]	λ_2 [nm]	$\Delta\lambda$ [nm]	$\Delta\phi_2$ [deg.]	$d_2 = \Delta\phi_2 \frac{\lambda_1\lambda_2}{4\pi\Delta\lambda}$	stage displacement
V	633.00	633.02	0.02	37.02	1.0301E+06	1000000 nm
VI	633.00	634.00	1.00	53.84	3.0010E+04	30000 nm
VII	632.60	637.96	5.36	0.11	1.2000E+01	12 nm
VIII	632.60	637.96	5.36	0	0.0000E+00	
						the step-height of the test sample is 1030012 nm

III. Set $\Delta\lambda$ to be a maximum and repeat the step I. The data $\Delta\phi_1$ is positive in this step, it means the position of the M_1 has not reached at W' and the TS should be moved forward 16 nm.

IV. The TS is moved back and forth until the condition $\Delta\phi_1$=0 is achieved as $\Delta\lambda$ is remained unchanged. Therefore, the M_1 is exactly positioned at W'.

The corresponding signals of steps I-IV display on the OSC are shown in Fig. 3(a)-(d) respectively.

Next, tune the SW to the position *b* for the Ray-2 and repeat the steps I~IV. Those steps are denoted as steps V~VIII for convenience. Finally, the M_1 is exactly positioned at G'. Because the points W' and G' are the corresponding positions of the top face of the gauge block and the wringing platen in the p-polarization arm of the interferometer, the difference of the readouts of the translation stage at Steps IV and VIII is equal to the step-height of the test sample and it is 1030012 nm in our test.

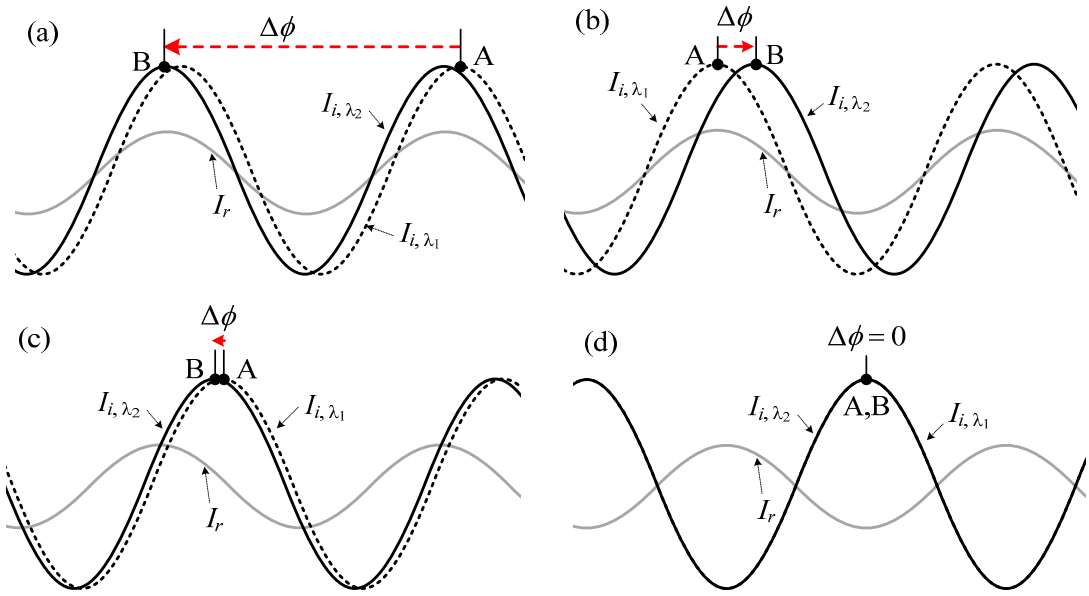

Fig. 3. The signals display on the oscilloscope for steps I-IV in our test.

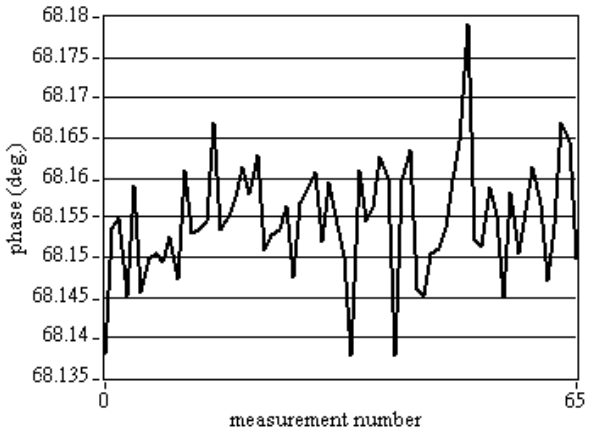

Fig. 4. The result of a data acquisition test of the phase-meter.

4. DISCUSSIONS

A data acquisition card (NI, PCI-6110) is installed in the phase-meter to acquire the sine wave signals of two photo-detectors, and the phases can be obtained with the three-parameter sine wave fitting (least squares fitting) technique [15]. The acquisition frequency of the card and the frequency difference of the heterodyne light source are 5 MHz and 500 Hz, respectively, so the theoretical phase uncertainty is 0.036° [16]. Fig. 4 shows the results of repeated phase measurements at a fixed experimental condition. Thus the experimental phase repeatability is about ±0.02°. The main two origins of the phase repeatability come from the instability of the laser power and the quantization noise. Because the phase measurement in this method is used only for identifying the absolute optical path difference position, the measurable range of this method is not limited by the coherence length of the light source. Although the displacement of the precision translation stage can be read with an optical meter inside the stage, its accuracy becomes worse for long distance measurements. It may have an error of 45 nm in a measured displacement of 100 mm. If a commercial laser interferometer such as Agilent 5529A is applied to directly measure the displacement of the reference mirror, then the measurement accuracy will be enhanced.

The measurement results reported in [17] show that the Abbe errors for reproducible wringing can be very small (less than 1 nm) for a high-quality 5 mm gauge block (Mitutoyo Company). If the displacement direction of the translation stage may not lie along the normal of the top surface of the gauge block, there is a guiding error of the translation stage. This error can be minimized ($< 1.2 \times 10^{-9} L$) when a goniometric cradle and a rotation stage with resolution of 10 arc second are applied in this system. If there is a parallelism error between Ray-1 and Ray-2 (30 arc sec. here), it will induce optical path errors in both two arms of the interferometer. Because the central fringe technique is used to identify zero optical path difference positions, these optical path errors can be eliminated each other.

Thus, the accuracy of the measurement result does not affected by the parallelism error. In addition, both the platen and the gauge block are made of steel, so there is no additional phase difference. If they are made of different materials, it may introduce an additional phase difference between the reflected lights from the platen and the gauge block face. It will affect the measurement results.

The uncertainty of this method mainly depends on the resolution δd_t (δd_t = 1 nm) of the TS and the uncertainty δd_c of the heterodyne central fringe identification technique. From Eq. (8), we have

$$\delta d_c = \frac{1}{4\pi\Delta\lambda}[\delta(\Delta\phi)\lambda_1\lambda_2 + \Delta\phi(\lambda_1\delta\lambda_2 + \lambda_2\delta\lambda_1) + \Delta\phi\lambda_1\lambda_2\frac{\delta(\Delta\lambda)}{\Delta\lambda}], \tag{9}$$

where $\delta(\Delta\phi)$ is the phase uncertainty of the PM, $\delta\lambda_i$ is the wavelength stability ($\delta\lambda_1 = \delta\lambda_2$), and $\delta(\Delta\lambda)$ is the resolution of the wavelength change. The first term represents the effect of phase uncertainty; the second and third terms are the effects of wavelength uncertainty. Because $\delta\lambda_1$ is much smaller than either λ_1 or λ_2, $\delta(\Delta\lambda)$ is also much smaller than $\Delta\lambda$, and $\Delta\phi$ can approach to $\delta(\Delta\phi)$, as d_i is nearly equivalent to 0, the second and the third terms can be neglected. Thus Eq. (9) can be simplified as

$$\delta d_c = \frac{\delta(\Delta\phi)\lambda_1\lambda_2}{4\pi\Delta\lambda}. \quad (10)$$

It can be seen that the effect of wavelength uncertainty can be ignored. By substituting the experimental conditions $\delta(\Delta\phi) = 0.036°$, $\lambda_1 = 632.6$ nm, $\lambda_2 = 637.96$ nm, and $\Delta\lambda = 5.36$ nm into Eq. (10), $\delta d_c \approx 3.8$ nm can be obtained. Therefore, the uncertainty of this method can be calculated as $\delta d_T = \left(\delta d_t^{\,2} + \delta d_c^{\,2}\right)^{1/2} \approx 4$ nm.

From Eq. (10), it is obvious that the increment of the tunable wavelength range will improve the accuracy of this method. The half-wave voltage of the EO needs to be adjusted for larger wavelength variations. In addition, the refraction index of air, the thermal expansion and the uncertainty of surface roughness of the gauge block should be considered in precise measurement [18-20].

5. CONCLUSIONS

A simple method for measuring a step-height sample has been presented with the heterodyne central fringe identification technique and a precision translation stage. This method can accurately point out the zero optical path difference position such that the optical path lengths of two arms of the interferometer are absolutely equivalent. Thus, the two surfaces of the step-height sample can be identified sequentially with the translation stage. The displacement of the translation stage is equal to the step-height of the test sample. The feasibility of the technique has been demonstrated. The measurable range is not limited by the coherence length of the light source and relates to the maximum travel range of the translation stage. The measurement accuracy depends on the uncertainties of the heterodyne central fringe identification method and the translation stage. In our setup, we have a 100 mm measurable range and a 4 nm uncertainty. The wavelength stability has a minor effect. Moreover, our technique has potential for application to the quality inspection of high aspect ratio MEMS/NEMS.

ACKNOWLEDGMENTS

This study was supported by the National Science Council, Taiwan, under contract NSC 98-2221-E-009-018-MY3.

REFERENCES

[1] Francon, M., [Optical interferometry], Academic, New York, 23-52 (1966).
[2] Haruna, M., Ohmi, M., Mitsuyama, T., Tajiri, H., Maruyama, H., and Hashimoto, M., "Simultaneous measurement of the phase and group indices and the thickness of transparent plates by low-coherence interferometry", Opt. Lett. 23, 966-968 (1998).
[3] Li, T., Wang, A., Murphy, K., and Claus, R., "White-light scanning fiber Michelson interferometer for absolute position-distance measurement", Opt. Lett. 20, 785-787 (1995).
[4] Dobosz, M., Matsumoto, H., Seta, K., and Iwasaki, S., "Polychromatic light interferometer for high-accuracy positioning", Opt. & Laser Eng. 24, 43-56 (1996).
[5] Hariharan, P. and Roy, M., "White-light phase-stepping interferometry: measurement of the fractional interference order", J. Mod. Opt. 42, 2357-2360 (1995).
[6] Ikonen, E. and Riski, K., "Gauge-block interferometer based on one stabilized laser and a white-light source," Metrologia 30, 95-104 (1993).
[7] Wang, Q., Ning, Y. N., Palmer, A. W., and Grattan, K. T. V., "Central fringe identification in white light interferometer using a multi-stage-squaring signal processing scheme", Opt. Commun. 117, 241-244 (1995).
[8] Lee, J. Y., Chiu, M. H., Su, D. C., "Central fringe identification using a heterodyne interferometric technique and a tunable laser-diode", Opt. Commun. 128, 193-196 (1996).
[9] Massie, N. A., Nelson, R. D. and Holly, S., "High-performance real-time heterodyne interferometry," Appl. Optics 18, 1797-1803 (1979).
[10] Gelmini, E., Minoni, U. and Docchio, F., "Tunable, double-wavelength heterodyne detection interferometer for absolute-distance measurements," Optics Lett. 19, 213-215 (1994).

[11] Chiu, M. H., Lee, J. Y., and Su, D. C., "Complex refractive-index measurement based on Fresnel's equations and the uses of heterodyne interferometry," Appl. Optics 39, 4047-4052 (1999).
[12] Chou, C., Kuo, W. C., and Han, C. Y., "Circularly polarized optical heterodyne interferometer for optical activity measurement of a quartz crystal," Appl. Optics 42, 5096-5100 (2003).
[13] Yariv, A. and Yeh, P., [Optical Waves in Crystal], Wiley, New York, p. 121 (1984).
[14] International organization for standardization, "Geometrical product specifications – length standards – gauge blocks," International Standard ISO 3650, (1998).
[15] IEEE, "Standard for terminology and test methods for analog-to-digital converters," IEEE Std. 1241-2000, 25-29 (2001).
[16] Chiu, M. H., Lee, J. Y. and Su, D. C., "Complex refractive-index measurement based on Fresnel's equations and the uses of heterodyne interferometry," App. Opt. 38, 4047-4052 (1999).
[17] Malinovsky, I., Titov, A., Massone, C., "Fringe-image processing gauge block comparator of high-precision," Proc. SPIE 3477, 92-100 (1998).
[18] Jin, J., Kim, Y. J., Kim, Y. and Kim, S. W., "Absolute length calibration of gauge blocks using optical comb of a femtosecond pulse laser," Opt. Express 14, 5968-5974 (2006).
[19] Lewis, A., "Measurement of length, surface form and thermal expansion coefficient of length bars up to 1.5 m using multiple-wavelength phase-stepping interferometry," Meas. Sci. Technol. 5, 694-703 (1994).
[20] Birch, K. P. and Downs, M. J., "An updated Edlen equation for the refractive index of air," Metrologia 30, 155-162 (1993).